ACTIVITY OF ALUMINA SUPPORTED Fe CATALYSTS FOR N$_2$O DECOMPOSITION: EFFECTS OF THE IRON CONTENT AND THERMAL TREATMENT

PABLO ALVAREZ[a], PAULO ARAYA[a], RENE ROJAS[b], SICHEM GUERRERO[c] AND GONZALO AGUILA[d,*]

[a]*Departamento de Ingeniería Química y Biotecnología, Facultad de Ciencias Físicas y Matemáticas, Universidad de Chile, Beauchef 851, Santiago, Chile.*
[b]*Facultad de Química, Pontificia Universidad Católica de Chile, Vicuña Mackenna 4860, Santiago, Chile.*
[c]*Facultad de Ingeniería y Ciencias Aplicadas, Universidad de los Andes, Monseñor Álvaro del Portillo 12455, Las Condes, Santiago, Chile.*
[d]*Departamento de Ciencias de la Ingeniería, Facultad de Ingeniería, Universidad Andres Bello, Antonio Varas 880, Santiago, Chile.*

ABSTRACT

The activity of Fe$_2$O$_3$/Al$_2$O$_3$ catalysts prepared by impregnation of Al$_2$O$_3$ with different amounts of Fe and calcination temperatures (650 and 900 ºC) in the direct N$_2$O decomposition reaction was studied. High calcination temperature was introduced to study the effect of "aging", which are the conditions prevailing in the process-gas option for N$_2$O abatement. The catalysts were characterized by BET, XRD, UV-DRS, and H$_2$-TPR. The incorporation of Fe promotes the alumina phase transition (γ-Al$_2$O$_3$ to α-Al$_2$O$_3$) when the catalysts are calcined at 900 ºC, which is accompanied by a decrease in the specific area. The activity of the catalysts and the specific surface area depend on Fe loading and calcination temperature. It was found that highly dispersed Fe species are more active than bulk type Fe$_2$O$_3$ particles. We conclude that Fe$_2$O$_3$/Al$_2$O$_3$ catalysts prepared by impregnation method are active in the decomposition of N$_2$O, to be used at low or high reaction temperatures (tail-gas or process-gas treatments, respectively), as part of nitric acid production plant.

Keywords: iron; alumina; impregnation method; N$_2$O decomposition

1. INTRODUCTION

N$_2$O is considered to be one of the gases with the largest contribution to the greenhouse effect, with a warming potential almost 300 times greater than that of CO$_2$ [1]. Plants that produce nitric acid are the largest generators of N$_2$O, which is an undesirable product of the catalytic oxidation of ammonia. Therefore, the abatement of N$_2$O is one of the main challenges from the standpoint of environmental protection.

There are different options for abating N$_2$O depending on where the catalytic process of N$_2$O decomposition is performed. It has been found that the best choices for existing plants, are locating the catalyst just under the Pt metal gauze in the ammonia burner (process-gas option), or in the tail-gas train (tail-gas option) [2]. In the first option, the catalyst must be able to withstand high temperatures, near 850 °C, while in the second the conditions and temperatures are more moderate and the catalyst must work at temperatures near 500-600 °C.

Most published papers refer to adequate catalysts for working with the tail-gas option, at moderate temperatures (500-600 ºC) and pressures of 1-3 bar. One of the most widely studied and with the best behavior is Fe supported on different kinds of zeolites [see 3-9, and references therein]. In fact, Uhde EnviNOx® markets a tail-gas option for removing N$_2$O and NOx that uses iron-containing zeolites [2]. In the Fe-zeolite system there is some degree of acceptance of surface iron species forming the core of the catalytic site, with the reaction mechanism involving the existence of an intermediate oxygen species called "α-oxygen" [10]. The proposed reaction mechanisms involve a Langmuir-Hinshelwood type [11, 12] as well as an Eley-Rideal type of mechanism [13, 14]. The surface migration and recombination of oxygen atoms to O$_2$ was found to be the rate limiting step [6]. Although there is some discrepancy on which is the active Fe species, it would be either extra-framework bare Fe^{2+} ions stabilized by Al^{3+} ions [9] or small Fe$_x$O$_y$ particles located inside the channel system [10].

However, the high temperatures and the presence of water prevent the use of systems based on zeolites directly in the combustion chamber of NH$_3$, due to their deactivation under hydrothermal conditions. Most of the catalysts that can be used in the process-gas option have been developed by catalyst producing companies. Some commercial catalysts for N$_2$O process-gas option decomposition are CuO/Al$_2$O$_3$ (BASF), La$_{0.8}$Ce$_{0.2}$CoO$_3$ (Johnson Matthey), Co$_2$AlO$_4$/CeO$_2$ (Yara International), and Fe Al$_2$O$_3$ (PKR2-INS) [2].

One of the few catalysts that are active at high temperatures and whose results have been published in the literature was reported by Giecko et al. [15], who showed that Fe$_2$O$_3$-Al$_2$O$_3$ catalysts prepared by coprecipitation of nitrate precursors of both metals can generate catalysts that are highly stable and active at high temperatures, under the conditions existing in the ammonia combustion chamber. The composition of the catalysts was varied between the mole ratios Fe/Al = 1.0 (41.8% Fe$_2$O$_3$ and 58.2% Al$_2$O$_3$ w/w) and Fe/Al = 3.5

(72.6% Fe$_2$O$_3$ and 27.4% Al$_2$O$_3$). The catalysts were calcined at 900 ºC and 1100 º for 5 h to simulate the aging in the reactor. According to these authors, the most active and stable catalyst contains the smallest amount of Fe$_2$O$_3$. The influence of the modifier (Al, Zr, Ce, La, Cu, and Cr) on the activity of the N$_2$O decomposition of catalysts with a constant content of 80% Fe$_2$O$_3$, prepared by coprecipitation was studied by Kruk et al. [16]. The catalysts were tested at a high temperature range (500 - 900 ºC). The activity sequence shows that it increases in the following order: Cr <Ce <Zr <La < Al <Cu, confirming that the Fe$_2$O$_3$-Al$_2$O$_3$ system is one of the most active for the N$_2$O decomposition reaction at high temperatures.

The system of Fe supported on Al$_2$O$_3$, prepared by impregnation of the Al$_2$O$_3$ support with the Fe precursor, has also been reported in the literature for the direct decomposition of N$_2$O. Several years ago, Pomonis et al. [17] reported the activity of Fe catalysts supported on alumina over a range of loads between 0.172 and 0.974 mmol of Fe per gram of alumina, equivalent to a low Fe load range between 0.96% and 5% (w/w), and for a moderate reaction temperature range of 500 to 650 ºC. They found that the catalytic activity is determined by the dispersion of Fe^{3+} and not by the nature of the Fe species on the surface of the support, either supported α-Fe$_2$O$_3$ particles or strongly associated Fe^{3+}. Some years later Kordulis et al. [18] studied the effect of the addition of Li to the alumina on the kinetics of the decomposition of N$_2$O in a series of supported Fe catalysts. The range of Fe loads and reaction temperatures used is similar to that reported in their previous work [17], and they found that the data fitted first order kinetics and that the addition of Li causes an important decrease of the catalyst's activity. The authors attribute the activity decrease by adding Li to a decrease of the dispersion of Fe and an increase of oxygen adsorptivity. Later, Chistotoforou et al. [19] studied the activity of the conversion of N$_2$O to N$_2$ on Rh, Ru, Pd, Co, Cu, Fe, and In catalysts supported on Al$_2$O$_3$, SiO$_2$, TiO$_2$, ZrO$_2$, and calcined hydrotalcite MgAl$_2$(OH)$_8$H$_2$O. The temperature range analyzed was between 200 and 650 ºC, and metal content between 1% and 2%. In the case of the alumina support, the activity sequence is Rh ≥ Ru > Fe > Pd > In > Co. More recently, Pekridis et al. [20] compared a series of metal catalysts (Pd, Rh, Ru, Cu, Fe, In, and Ni) supported on γ-alumina, with a fixed load of 2% (w/w) in the decomposition of N$_2$O in the presence and absence of O$_2$ and reducing agents. They found that the activity sequence is the same with or without O$_2$: Ru ≥ Pd ≥ Rh > Cu > Fe > In > Ni. The temperature range used was moderate, between 200 ºC and 600 ºC.

It can therefore be concluded that Fe$_2$O$_3$/Al$_2$O$_3$ catalysts prepared by impregnation are active systems for the decomposition of N$_2$O. However, they have been studied in a moderate temperature range (less than 650 ºC), making them adequate, in principle, for the tail-gas option.

Considering the good behavior of the Fe$_2$O$_3$-Al$_2$O$_3$ catalysts prepared by coprecipitation [15], it is reasonable to assume that the Fe$_2$O$_3$/Al$_2$O$_3$ catalysts prepared by impregnation of the support can also be applicable to high temperature conditions. Therefore, the present work explores the feasibility of

e-mail: gonzalo.aguila@unab.cl

using catalysts of Fe supported on alumina for the high temperature range, similar to that used in the process-gas option. An advantage that the catalysts prepared by impregnation of alumina can have, is that larger specific areas than those generated by the coprecipitation method can be obtained, allowing better dispersion of the Fe on the surface of the catalyst. On the other hand, the available commercial alumina pellets would facilitate the eventual preparation of commercial catalysts and further lowering the costs.

For that purpose a study is made of the effect of the Fe load (between 10% and 50% w/w) and the calcination temperature of the catalyst (650 ºC and 900 ºC) on the decomposition activity of N_2O by Fe catalysts supported on commercial alumina. The catalyst's calcination at 900 ºC is used to simulate a catalyst's aging when exposed to the high temperatures required in the process-gas option.

2. MATERIAL AND METHODS

The catalysts were prepared by dry impregnation of the γ-Al_2O_3 (Sigma-Aldrich) support with an aqueous solution of iron(III) nitrate nonahydrate (Merck, p.a.), with the adequate content of precursor to obtain Fe loads between 10% and 50% (w/w) with respect to the support. After the impregnation with the precursor, the material was dried in an oven at 105 ºC overnight, and then it was calcined in a muffle furnace at 650 ºC for 3 h. One part of this catalyst, already calcined at 650 ºC, was then calcined at 900 ºC for additional 3 hours. The prepared catalysts are identified as "CAT X-Fe-Y", where X indicates the Fe load and Y is the catalyst's final calcination temperature.

Besides the supported catalysts, the characteristics and catalytic behavior of the unsupported Fe_2O_3 were studied. Commercial Fe_2O_3 (Sigma Aldrich, p.a.) was used for this purpose; it was calcined at 650 ºC for 3 h, and part of it was further calcined at 900 ºC for 3 h to emulate the treatment to which the supported Fe_2O_3 catalysts would be subjected.

The samples were characterized by N_2 adsorption, X-ray diffraction (XRD), UV-diffuse reflectance spectra (UV-DRS), and temperature programmed reduction in a hydrogen stream (TPR).

Determination of the specific surface area of the catalysts was made measuring the N_2 adsorption in a Micromeritics sorptometer, Model ASAP 2010. The samples were previously degassed at 200 ºC.

The crystal structure of the different catalysts was determined on a Siemens D-5000 diffractometer using Cu Kα radiation and a scan rate of 0.02 degrees per minute. In order to calculate the crystallite size of Fe_2O_3, the Scherrer equation was used (Equation 1).

$$t = \frac{K \cdot \lambda}{B \cdot \cos\theta} \qquad (Eq.\,1)$$

In Equation 1, t is the mean crystallite size of Fe_2O_3 (in Å), K is the Scherrer constant (0.9), λ is the wavelength of the X-ray (1.54178 Å), and B is the width of the diffraction peak at a height half-way (Full Width at Half Maximum, FWHM) located at 2θ (in radians).

The UV–DRS analyses were made on a Perkin Elmer Lambda 650 instrument equipped with a Praying Mantis and a Harrick powder cell.

Finally, the temperature programmed reduction analyses were made on a conventional system equipped with a TCD detector, with a flow of 20 cm³/min of a gaseous mixture of 5% H_2 in Ar at a heating rate of 10 °C/min between ambient temperature and 700 ºC. The amount of catalyst loaded in the reactor was adjusted so that it always contained the same mass of Fe, which will be justified in the respective TPR characterization analysis section. The hydrogen consumption was determined using a conversion factor, which allows the area under the TPR curve to be directly transformed into consumed H_2 moles. This conversion factor was estimated through an experiment of a 100 uL H_2 pulse produced by a loop valve installed on the same TPR equipment. Considering an ideal gas, 100 uL of H_2 can be transformed into moles of H_2. By integrating the area under the curve of the pulse of 100 uL H_2 and considering the calculated amount of H_2 moles in this pulse, the conversion factor can be obtained.

The catalytic activity tests were performed in a piston flow tubular reactor, with a flow of 5000 ppm N_2O balanced in He, at a total flow rate of 100 cm³/min, operated at atmospheric pressure. After loading the reactor with 0.35 g of catalyst, the catalyst was pretreated at 400 ºC with O_2 for 30 min and then at 600 ºC for 1 h with He. After the pretreatment, the reactor temperature was decreased to 400 ºC, and the reactant (N_2O balanced in He) was then fed to the reactor. After 30 min of N_2O flow, the temperature was increased from 400 ºC to 600 ºC, taking samples every 25 ºC to determine the concentration of N_2O

on a Perkin Elmer Autosystem chromatograph equipped with a HAYASEP D column and a TCD detector. The N_2O conversion (X) was calculated according to Equation 2.

$$X = \frac{[N_2O]_{in} - [N_2O]_{out}}{[N_2O]_{in}} \qquad (Eq.\,2)$$

3. RESULTS AND DISCUSSION

3.1. Characterization of the materials
3.1.1. Specific BET area

The specific surface area results of the supports and the catalysts with different Fe loads calcined at 650 ºC and 900 ºC are shown in Table 1, which also includes the specific surface areas of the commercial iron oxide calcined at 650 ºC (4 m²/g) and 900 ºC (1 m²/g).

Table 1. BET surface areas and crystallite size of Fe supported on alumina catalysts.

Catalyst	Details	BET area (m²/g)	Crystallite size of Fe_2O_3 (Å)
Alumina-650	Pure support calcined at 650 ºC	128	-
CAT 10-Fe-650	10% Fe calcined at 650 ºC	110	n.d.
CAT 20-Fe-650	20% Fe calcined at 650 ºC	95	145
CAT 30-Fe-650	30% Fe calcined at 650 ºC	78	178
CAT 40-Fe-650	40% Fe calcined at 650 ºC	74	176
CAT 50-Fe-650	50% Fe calcined at 650 ºC	75	165
Fe_2O_3-650	Commercial Fe_2O_3 calcined at 650 ºC	4	203
Alumina-900	Pure support calcined at 900 ºC	65	-
CAT 10-Fe-900	10% Fe calcined at 900 ºC	28	n.d.
CAT 20-Fe-900	20% Fe calcined at 900 ºC	9	173
CAT 30-Fe-900	30% Fe calcined at 900 ºC	12	187
CAT 40-Fe-900	40% Fe calcined at 900 ºC	17	201
CAT 50-Fe-900	50% Fe calcined at 900 ºC	33	211
Fe_2O_3-900	Commercial Fe_2O_3 calcined at 900 ºC	1	254

n.d.: not detected

It is seen that when the catalyst is calcined at 650 °C, the increase of the Fe loading from 10% to 30% causes a decrease of the specific surface area with respect to that of the pure alumina support. Beyond 30%, the specific surface area of the catalyst changes slightly.

As the calcination temperature is increased up to 900 °C, all the catalysts decreased their specific surface area with respect to those calcined at 650 °C, which, as will be seen later, is essentially due to the phase change from γ-alumina into α-alumina. As the Fe load is increased, the specific surface area of the catalysts calcined at 900 °C goes through a minimum (CAT 20-Fe-900). This behavior is not easy to explain, and it is being the subject of a specific study to elucidate this issue.

3.1.2. X-ray diffraction (XRD)

Figures 1(A) and 1(B) show the XRD results of the catalysts calcined at 650 ºC and 900 ºC, respectively. Both figures include the diffractogram of pure alumina and commercial iron oxide calcined at those temperatures.

The usual XRD analysis of pure alumina should show characteristic peaks of γ-alumina at 35.5º, 45.7º and 66.6º (JCPDS 50-0741). However, Figure 1(A) shows that the most intense peaks for γ-alumina support are those located at 45.7º and 66.6º. On the other hand, the diffractogram of commercial iron oxide, also calcined at 650 °C, shows the characteristic peaks of α-Fe_2O_3 at 33.2º, 35.6º, 49.4º, 54.1º, 62.4º and 63.9º (JCPDS 80-0550). When impregnated with 10% Fe, CAT 10-Fe-650, it is seen that the intensity of the peaks corresponding to γ-alumina drops substantially, and the peaks corresponding to α-Fe_2O_3 start appearing. The decrease of the intensity of the γ-alumina peaks with 10% Fe load is greater than expected from a simple dilution of the alumina with Fe, and suggests that the Fe decreases the crystallinity of the support, probably related to the diffusion of Fe in the alumina structure. In fact, Colaianni et al. [21] have reported that Fe can diffuse in the alumina at temperatures above 627 ºC. As the Fe load is increased to 20%, CAT 20-Fe-650, the peaks corresponding to α-Fe_2O_3 increase their intensity substantially, reflecting an important increase of the concentration and/or crystallinity of the Fe_2O_3 particles. At the same time, the intensity of the peaks of γ-alumina decrease even more.
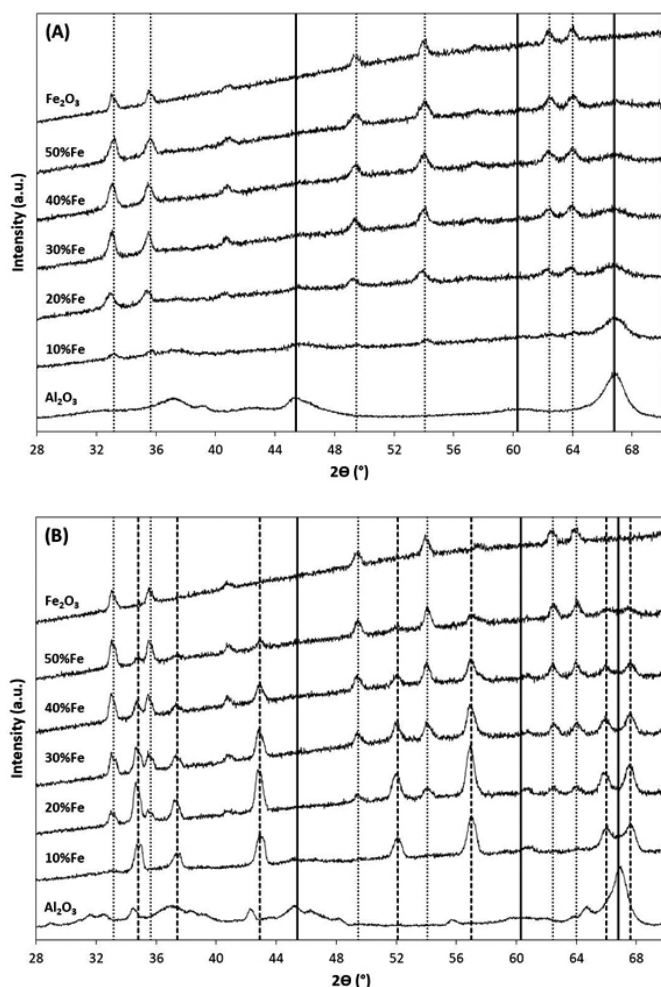

Figure 1. XRD results for Fe/Al_2O_3 catalysts with different Fe loads and calcination temperatures: (A): 650 °C; (B): 900 °C. The main characteristic diffraction lines of γ-Al_2O_3 (———), α-Al_2O_3 (- - - - -), and α-Fe_2O_3 (·······) are included.

Increasing the Fe load to 30% also causes a substantial increase of the intensity of the peaks of α-Fe_2O_3, indicating that the concentration and/or crystallinity of the Fe_2O_3 particles continue to increase. However, the intensity of the peaks corresponding to γ-alumina remains constant. Curiously, greater Fe

loads, CAT 40-Fe-650 and CAT 50-Fe-650, no longer generate higher intensity of the α-Fe_2O_3 peaks, and the intensity of the peaks of γ-alumina remain constant. This suggests that above 30% the greater Fe load does not cause an increase of the concentration, size, or crystallinity of α-Fe_2O_3. Apparently, Fe would form amorphous Fe_2O_3 particles not detectable by XRD. Table 1 also includes the calculated crystallite size of the Fe_2O_3 using the Scherrer equation (see Equation 1) and the peak diffraction located at 2θ = 54.1º, showing that the size of the α-Fe_2O_3 particles is randomly around 162 Å over the whole range of Fe loads, showing that the α-Fe_2O_3 particles do not increase in size with increasing Fe load. What should also be noted in Table 1 is that the crystallite size of the commercial Fe_2O_3 is small (around 203 Å), which is only slightly larger than that found in the supported catalysts.

Figure 1(B) shows that when the alumina support is calcined at 900 ºC it undergoes a considerable alteration. The alumina previously calcined at 650 °C, which is practically γ-Al_2O_3, when calcined at a high temperature is transformed into a polymorphic mixture whose maxima can be associated with γ-Al_2O_3 (JCPDS 50-0741), non-stoichiometric alumina (JCPDS 79-1559), κ-Al_2O_3 (JCPDS 52-0803), and α-Al_2O_3 (JCPDS 50-1496). In fact, the specific surface area of the alumina calcined at 650 ºC (128 m^2/g) drops to approximately one half when calcined at 900 ºC (68 m^2/g), which is consistent with an important structural change of the alumina. When loaded with 10% Fe, CAT 10-Fe-900, the diffractogram shows important changes with respect to those found for the catalyst with the same load calcined at 650 ºC and to the diffractogram of the support alumina calcined at 900 °C. Calcination at high temperature (900 °C) and 10% Fe jointly leads to the appearance of intense peaks corresponding to the formation of the α-alumina phase (considering JCPDS 50-1496, with 2θ = 35.0º, 43.2º and 57.2º). Clearly, the presence of Fe favors the phase transition from γ-alumina to α-alumina when calcining at 900 ºC. This result agrees with literature reports [22, 23]. In fact, Zhong et al. [22] show the complete transformation of γ-alumina into α-alumina at 1000 ºC in iron oxide-coated alumina, while this transformation does not occur in pure alumina calcined at the same temperature. On the other hand, Li et al. [23] also show the transformation into α-alumina of a catalyst with 25% Fe supported on γ-alumina when it is calcined at 900 ºC for 3 h. As seen in Figure 1(B), in the CAT 10-Fe-900 the Fe species must be highly dispersed, because diffraction peaks associated with α-Fe_2O_3 are not visible. As the Fe load is increased to 20%, the diffractogram of the CAT 20-Fe-900 catalyst shows an increased intensity of the peaks corresponding to α-alumina, and the peaks corresponding to α-Fe_2O_3 can be identified. For 30% and greater Fe loads the diffractograms are characterized by an increase of the intensity of the peaks due to α-Fe_2O_3, while the peaks associated with α-alumina decrease their intensity. Another aspect that should be highlighted is that calcination at higher temperatures causes only a moderate increase of the crystallite size of supported as well as unsupported Fe_2O_3, as shown in Table 1. Therefore, the supported catalysts increase their particle size from an average of 166 Å to an average of 193 Å, while unsupported Fe_2O_3 increases its size from 203 Å to 254 Å.

3.1.3. UV-diffuse reflectance spectra (UV-DRS)

The UV-DR spectra of the different catalysts are presented in Figure 2. In order to facilitate the observation of electronic changes within the spectra of each catalyst when calcined at high temperatures, the spectra of the catalyst calcined at 650 °C (dotted line) and 900 °C (continuous line) are included. For comparison purposes, the UV-DR spectra of commercial Fe_2O_3 is also included.

In the literature there is plentiful information for the interpretation of the UV-DR spectra of Fe catalysts on different types of zeolites [5, 24, 25, 26]. According to these reports, the 200-300 nm zone can be assigned to isolated Fe^{3+} ⟵ O charge-transfer (CT) bands. The 300-450 nm zone corresponds to Fe^{3+} ions in small oligonuclear clusters, and bands above 450 nm are characteristic of larger Fe_2O_3 particles. In the case of iron oxide supported on alumina the literature is scarce, subsequently the band assignment is based on the analogy with those from Fe-Zeolite [27, 28].

In general, Fe supported on Al_2O_3 catalysts calcined at 650 °C show bands that can be associated with isolated Fe^{3+} species below 300 nm, oligonuclear species between 300 and 450 nm, and bulk Fe_2O_3 particles above 500 nm at different relative concentrations. On the contrary, the spectra of commercial Fe_2O_3 shows a strong decrease of the absorbance below 300 nm, indicating that there are no isolated Fe^{3+} species. Obviously, these kinds of species cannot exist in unsupported Fe_2O_3.
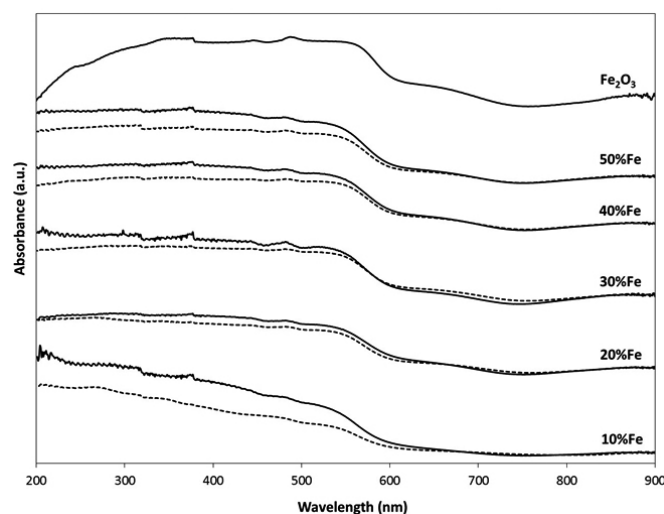
Figure 2. UV-DRS results for the Fe/Al_2O_3 catalysts with different Fe loads and calcination temperatures: 650 °C (―――――) and 900 °C (·······).

The UV-DR spectra of CAT 10-Fe-650 catalyst shows a continuous increase of the intensity as the wavelength decreases from about 550 nm to 200 nm, indicating that the relative concentration of the oligonuclear species and of isolated Fe^{3+} is high in this catalyst. As the load is increased to 20%, CAT 20-Fe-650, it is seen that the zone below 450 nm is flattened, indicating a decrease of the relative concentration of isolated Fe^{3+} species and an increase of oligonuclear Fe_2O_3 species and particles. This is consistent with an increase of the intensity of the diffraction peaks of the crystalline Fe_2O_3 particles, shown in Figure 1(A) for CAT 20-Fe-650 catalyst. After a 30% load of Fe, the UV-DR spectra shows a slight increase of the absorbance in the zone above 500 nm, indicating the formation of bulk Fe_2O_3 particles. With these loads, the zone below 500 nm is relatively similar for these catalysts, indicating that the relative concentration of the oligonuclear and isolated Fe^{3+} species does not vary substantially.

Regarding the catalysts calcined at 900 °C and compared to those calcined at lower temperature (650 °C), in the case of CAT 10-Fe-900 an important decrease of the absorbance is seen below 600 nm. However, the shape of the absorption curve is similar to that of the catalyst calcined at 650 ºC, and it is characterized by a continuous increase of the absorption as the wavelength drops below 550 nm. The largest difference is seen under 300 nm, where the curve is flattened, indicating a decrease in the relative concentration of the isolated Fe^{3+} species with respect to CAT 10-Fe-650 catalyst. In the CAT 20-Fe-900 catalyst, higher calcination temperature does not produce important changes with respect to CAT 20-Fe-650 catalyst. The main difference is seen in the 300 to 450 nm zone, where the absorbance decreases slightly in CAT 20-Fe-900 catalyst, indicating a decrease of the relative concentration of oligonuclear Fe species. For catalysts with greater loads, although there is a decrease of the absorbance in the zone between 200 and 600 nm, that decrease is still more pronounced in the zone below 300 nm, suggesting that the concentration of the isolated Fe^{3+} species is affected more strongly by the calcination at 900 ºC than the concentration of the oligonuclear species. Therefore, it can be concluded that calcination at 900 ºC causes mainly a decrease of the isolated Fe^{3+} species, but the relative concentration of the other Fe species on the surface is not substantially affected by the calcination at high temperature.

3.1.4. Temperature programmed reduction (TPR)

The TPR curves for the different catalysts are shown in Figure 3 and the corresponding H_2 consumption is given in Table 2. In the same way as in the UV-DRS analysis (Figure 2), the TPR curves of catalyst calcined at 650 °C and 900 ºC, dotted and continuous lines, respectively, are included. For comparison purposes, the TPR of commercial Fe_2O_3 is also included.
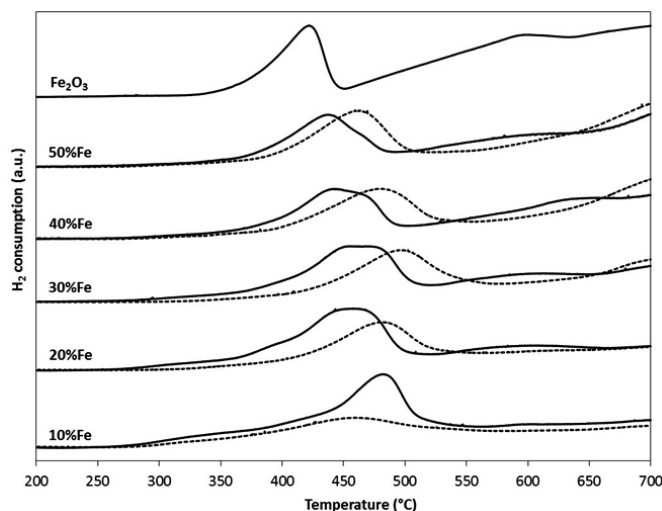

Figure 3. H_2-TPR results for the Fe/Al_2O_3 catalysts with different Fe loads and calcination temperatures: 650 °C (―――――) and 900 °C (·······).

The reduction of unsupported Fe_2O_3 has been studied in the literature, and it is arguable whether it occurs in two steps: $Fe_2O_3 \rightarrow Fe_3O_4 \rightarrow Fe^0$ [29, 30] or in three steps: $Fe_2O_3 \rightarrow Fe_3O_4 \rightarrow FeO \rightarrow Fe^0$ [31, 32]. This controversy has been approached by Zielinski et al. [33], who postulate that the number of steps depends on the relation between the concentration of H_2 and the amount of water present during the reduction (X_{H2O}/X_{H2} ratio). At low X_{H2O}/X_{H2} ratios (less than 0.35), the Fe_2O_3 is reduced in two steps, giving rise to the so-called α and β peaks. The α peak occurs at temperatures close to or less than 450 ºC, and it corresponds to the reduction of Fe_2O_3 to Fe_3O_4, while the higher temperature peak, β peak, occurs at a maximum close to or greater than 500 ºC, and it corresponds to the reduction of Fe_3O_4 to Fe^0. At high X_{H2O}/X_{H2} ratios (greater than 0.35) the reduction should occur in three steps, giving rise to an α peak with a maximum close to 450 ºC, a $β_1$ peak with a maximum close to 600 ºC which corresponds to the Fe_3O_4 to FeO step, and a $β_2$ peak with a maximum above 800 ºC that corresponds to the FeO to Fe^0 step.

Table 2. H_2 consumption from catalysts during TPR experiments expressed as number of H_2 moles consumed per mol of Fe_2O_3 loaded in the reactor. The stoichiometric number of H_2 moles required to reduce Fe_2O_3 to Fe_3O_4 is 0.33, Fe_2O_3 to FeO is 2, and Fe_2O_3 to Fe^0 is 3, all of them calculated per mole of Fe_2O_3.

Catalyst	Moles of H_2 consumed per mole of Fe_2O_3
Fe_2O_3-650	1.2
CAT 10-Fe-650	0.6
CAT 20-Fe-650	0.7
CAT 30-Fe-650	0.7
CAT 40-Fe-650	0.8
CAT 50-Fe-650	0.9
Fe_2O_3-900	1.2
CAT 10-Fe-900	0.4
CAT 20-Fe-900	0.5
CAT 30-Fe-900	0.6
CAT 40-Fe-900	0.8
CAT 50-Fe-900	0.9

In the case of the reduction with H_2 of Fe_2O_3 supported on alumina, there is scarce literature, and the interpretation of the TPR curve is more complicated. Michorczyk et al. [34] suggest that the presence of alumina stabilizes the Fe_2O_3 phase and the reduction goes through the formation of $FeAl_2O_4$, whose reduction would occur above 700 ºC. Giecko et al. [15] interpret their TPR curve of Fe_2O_3/Al_2O_3 catalysts assuming that the reduction takes place in two steps, with a peak in the 450-530 ºC zone, attributed to the reduction of Fe_2O_3 to Fe_3O_4 and a second peak between 750 and 850 ºC attributed to the reduction of Fe_3O_4 or $FeAl_2O_4$ to Fe^0. In other cases [35], however, the TPR curve of supported Fe_2O_3 is interpreted using the reduction scheme proposed by Zielinski et al. described above [33].

Based on literature reports mentioned above and under the experimental conditions used in the present work, it would be expected that that the reduction should take place in three steps. In order to maintain the X_{H2O}/X_{H2} ratio fixed, the same mass of Fe was used in the TPR experiments, which was attained by varying the mass of catalyst loaded in the reactor. Therefore, the number of H_2 moles consumed by each catalyst, expressed per mole of Fe_2O_3 loaded in the reactor, is tabulated in Table 2.

Considering the catalysts calcined at 650 °C, CAT 10-Fe-650, it shows that the reduction begins at 300 ºC, reaching a maximum at around 480 ºC. According to literature this maximum can be assigned to the α peak, which corresponds to the reduction of Fe_2O_3 to Fe_3O_4. Therefore, the H_2 consumption by the CAT 10-Fe-650 catalyst is consistent with this assignment. In fact, Table 2 shows that the number of H_2 moles consumed by the CAT 10-Fe-650 catalyst is higher than the amount of H_2 needed to reduce Fe_2O_3 to Fe_3O_4 (0.33), but smaller than the amount needed to completely reduce Fe_2O_3 to FeO (2.0). The latter can also be observed in Table 2 for the rest of the catalysts in this study. Therefore, it is expected that a mixture of Fe_3O_4 and FeO species to be present after the TPR experiment in all the catalysts.

The TRP curve of CAT 20-Fe-650 catalyst present the α peak broadens and it is difficult to assign a maximum, but clearly the reduction occurs at lower temperature (around 460 ºC) with a second peak starting appearing at around 600 ºC, as show in Figure 3. This second peak can be assigned to peak β_1 described by Zielinzki et al. [33], and it reflects the reduction of Fe_3O_4 to FeO. This catalyst's H_2 consumption increases slightly with respect to CAT 10-Fe-650 catalyst (0.7 > 0.6, respectively), indicating that the number of species and their reducibility is greater in the 20-Fe-650 catalyst. As the load is increased to 30%, CAT 30-Fe-650 catalyst, the α peak tends to divide into two peaks, probably due to the formation of particles of different size, with maxima at 455 ºC and 470 ºC. At the same time, H_2 consumption do not change, indicating that there is no increase or decrease of the concentration of species reducible up to 700 ºC. The TPR curve of CAT 40-Fe-650 catalyst shows two reduction maxima peaks are seen at 440 and 464 ºC, while H_2 consumption increases slightly with respect to CAT 30-Fe-650 catalyst (0.8 > 0.7, respectively). For CAT 50-Fe-650 catalyst, the slope of the TPR curve increases steeply and it gets similar to the reduction curve of pure commercial Fe_2O_3, included in Figure 3. Obviously, the maximum attributable to peak β_2, which corresponds to the reduction of Fe_3O_4 (or of $FeAl_2O_4$) to Fe, cannot be seen in these experiments, since it would take place at temperatures close to 800 ºC. In this CAT 50-Fe-650 catalyst the α peak is transformed into a single peak with a reduction maximum at 437 ºC, the lowest temperature of the whole series of supported catalysts. Its H_2 consumption increases slightly at 0.9 moles of H_2 consumed per mole of Fe_2O_3 (see Table 2), indicating that this catalyst has the highest and most reducible number of species of the whole catalysts calcined at 650 °C. The TPR curve of pure Fe_2O_3 shows that the reduction α peak occurs at the lowest temperature and the consumption of H_2 is the highest (1.2), indicating that supported Fe oxide is more easily reduced than when it is supported on alumina.

The TPR curves of catalysts calcined at 900 ºC are also shown in Figure 3. When the TPR curves CAT 10-Fe-650 catalyst are compared with CAT 10-Fe-900 catalyst, a decrease of H_2 consumption and a displacement of the α peak maximum to lower temperature are seen. In fact, Table 2 shows that the H_2 consumption decreases from 0.6 to 0.4 moles of H_2 consumed per mole of Fe_2O_3 when catalyst it is calcined at 900 ºC, while the temperature of the α peak maximum is displaced from 480 ºC to 460 ºC, indicating that although there is a decrease of the number of reducible sites up to 700 ºC, these sites are easier to reduce. As the load is increased to 20%, H_2 consumption also decreases as the temperature increases, as shown in Table 2. However, in contrast with the case with 10% Fe, the maximum of the α peak is displaced to a higher temperature in the catalyst calcined at 900 ºC, indicating that the concentration of sites and their reducibility decrease with the higher calcination temperature. As the load is increased to 30%, the temperature of the maximum H_2 consumption corresponding to the α peak is still higher than that of the catalyst calcined at 650 ºC. This maximum is displaced to a higher temperature than in the

catalysts with lower Fe loadings. As the Fe load is increased from 30% to 40%, both calcined at 900 ºC, the maximum H_2 consumption of the α peak shifts to a lower temperature. In both cases, the temperature of the α peak is higher than the catalyst with the same loadings calcined at 650 ºC. At the same time, the areas under the curves of the catalysts calcined at 650 ºC and 900 ºC are almost the same, as seen in Table 2. This indicates that the concentration of reducible sites does not vary upon calcining at 650 ºC and 900 ºC, although their reducibility decreases slightly as the calcination temperature increases. In the catalyst with a 50% load of Fe, CAT 50-Fe-900, the α peak also moves to a higher temperature than CAT 50-Fe-650. However, compared with the catalyst with 40% Fe, this temperature difference is smaller. On the other hand, the consumption of H_2 is the same as with the catalyst calcined at 650 ºC, i.e. 0.9 moles of H_2 consumed per mole of Fe_2O_3 for both catalysts. It can therefore be concluded that the catalyst with 50% Fe is the one whose reducibility is least affected when it is calcined between 650 ºC and 900 ºC.

It should be noted that regardless of the load and the calcination temperature, the reducibility of Fe supported on alumina is less than that in pure Fe_2O_3. Therefore, alumina has a stabilizing role on the Fe^{3+} ions, making their reduction more difficult. This is seen clearly in Table 2, which shows that the consumption of H_2 by Fe_2O_3 below 700 ºC is higher than all the Fe catalysts supported on alumina.

3.2. Catalyst activities

Figures 4(A) and 4(B) show the N_2O conversion vs. temperature plots of the catalysts with different loads of Fe calcined at 650 and 900 ºC, respectively. The activity of the catalysts was study in the so-called moderate range of temperature from 400 up to 600 °C. As seen in Figure 4(A), when the catalysts are calcined at 650 ºC, the conversion substantially increases as the Fe load is increased from 10% to 20%, CAT 10-Fe-650 and CAT 20-Fe-650, respectively. However, when the load is increased to 30% the conversion decreases, showing that there is a maximum of activity around 20% Fe load. When the Fe load is increased to 40% and 50%, the conversions are basically the same, with both catalysts showing lower activity than that with 20% Fe load. The latter reaffirms the existence of a maximum in the conversion for the CAT-20-Fe-650 catalyst. In summary, the activity of the catalysts calcined at 650 ºC can be ordered in terms of Fe loading as: 20% > 30% > 40% ≈ 50% > 10%.

In the literature on catalysts of Fe supported on zeolites [13, 24-26], it is stated that the Fe species can be found in three main forms: isolated Fe^{3+} species, oligomeric species formed by small clusters (dimers or clusters of few Fe atoms), and bulk type Fe species. Although most reports recognize that the controlling step in the decomposition of N_2O is the recombination of oxygen atoms, the activity of each of these species is a controversial issue. Kondratenko et al. [13] state that excluding the large Fe_2O_3 clusters, all these species may have some activity in the direct decomposition of N_2O reaction.

On the other hand, Pérez-Ramírez et al. [36] suggest that the oligomeric Fe species may be more active than the isolated Fe species, since oxygen recombination is easier in the Fe clusters. Nobukawa et al. [37] even postulate that at least dimers are required to catalyze the decomposition of N_2O. In contrast, Hayden et al. [14] suggest that isolated iron cation species are responsible for the decomposition of N_2O. Pringruber et al. [6] concluded that the activity depends on the self-reduction capacity of the catalyst during the pretreatment with He, and that it decreases in the order: monomers > dimers > oligomers > Fe_2O_3 particles. It is during the treatment with He that the Fe^{2+} sites required to catalyze the reaction are generated. Sazama et al. [38] propose that Fe^{2+} ions and dimeric (Fe^{2+}-O-Fe^{2+}) complexes would be the most active for the decomposition of N_2O, and they are stabilized by the Al^{3+} lattice or by an extra Al^{3+} framework as proposed by Wang et al. [39].

In our Fe supported on alumina catalysts calcined at 650 ºC the UV-DRS analysis show, in general, the presence of the three types of species in different relative concentrations depending on the Fe load. In fact, in the CAT 10-Fe-650 and CAT 20-Fe-650 catalysts the UV-DR spectra show that the relative concentration of isolated Fe^{3+} species clearly decreases as the Fe load increases from 10% to 20% Fe, while the concentration of oligonuclear species and bulk Fe_2O_3 species increase their concentration. The XRD diffractogram of both catalysts are consistent with the observation of an increase of bulk Fe_2O_3 species, because in the CAT 10-Fe-650 catalyst the peaks associated with α-Fe_2O_3 are barely perceptible, while the intensity of these peaks increases considerably as the load increases to 20% in CAT 20-Fe-650. Since the bulk Fe_2O_3 species are considered almost inactive, the catalyst's increased activity with 20% Fe, CAT 20-Fe-650, would be due essentially to an increase in the total amount of the oligonuclear Fe species. It must be kept in mind that the Fe load is duplicated in the CAT 20-Fe-650 catalyst with respect to that in CAT

10-Fe-650, so even if the relative concentration of oligonuclear Fe species had not increased in CAT 20-Fe-650, the total number of these species would have increased, because the catalyst mass loaded in the reactor is the same. We will go back to this point later when we analyze the value of the kinetic constants of these catalysts. On the other hand, as discussed previously, the reducibility of CAT 20-Fe-650 is greater than that of CAT 10-Fe-650, and this is also an effect that contributes to increase the activity of CAT 20-Fe-650 because it is related to the lability of oxygen and the ease for creating Fe^{2+} sites [40]. The BET specific surface area decreases moderately from 110 m^2/g to 95 m^2/g as the Fe load increases from 10% to 20%, so the total surface area is not expected to have an important role in the activity of these two catalysts.
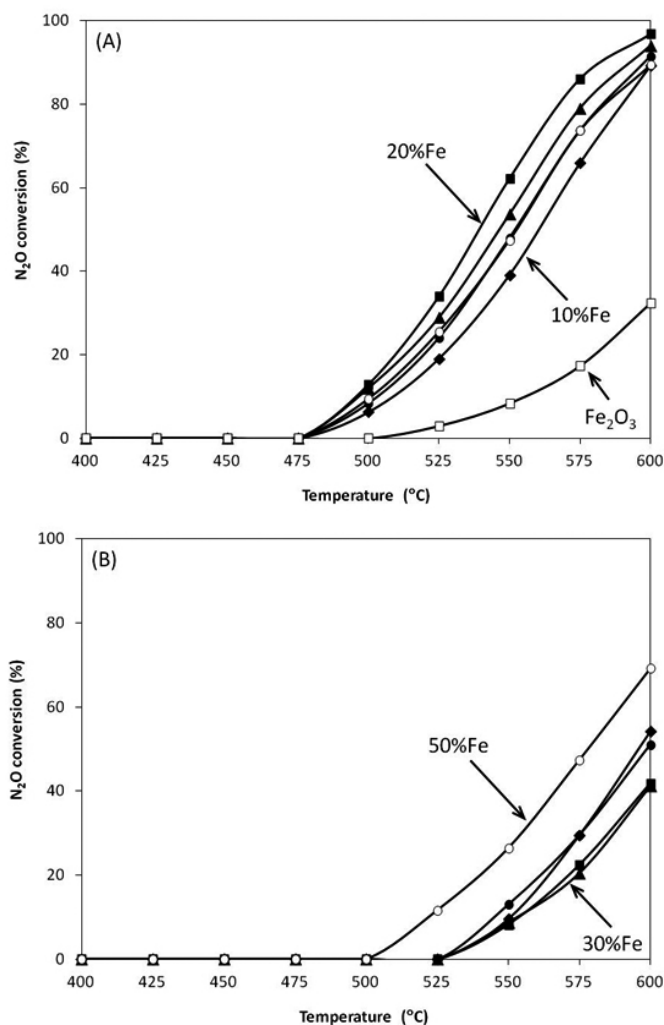

Figure 4. Activity in N_2O conversion for Fe/Al_2O_3 catalysts with different Fe loads: (♦) 10%Fe, (■) 20%Fe, (▲) 30%Fe, (●) 40%Fe, (○) 50%Fe and (□) Fe_2O_3, and calcination temperatures: (A): 650 °C; (B): 900 °C.

When the load is increased to 30%, CAT 30-Fe-650 catalyst, the conversion decreases slightly with respect to that found with the catalyst with the lowest load, CAT 20-Fe-650. This indicates that either the total number of catalytic sites decreases or its activity decreases with the increasing load of Fe to 30%. Comparing the UV-DR spectra of CAT 20-Fe-650 and CAT 30-Fe-650, there is an increase of bulk Fe_2O_3 species also confirmed by XRD, which shows an increased intensity of the α-Fe_2O_3 peaks, particularly those at 2θ = 33.2º and 35.6º. On the other hand, the TPR experiments show that the reduction peak, which in CAT 20-Fe-650 appears with a maximum around 460 ºC, is divided into two peaks with maxima at 453 ºC and 470 ºC. Therefore, the reducibility of CAT 30-Fe-650 is less than that of CAT 20-Fe-650. Moreover, the BET specific surface area drops from 95 m^2/g to 78 m^2/g as the Fe load increases, so all the characterization techniques point at the formation of a lower activity

catalyst as the load increases from 20 to 30% Fe. Clearly, in CAT 30-Fe-650 the increase of the total amount of Fe does not make up for the loss of activity of the Fe species.

At higher loads of 40% and 50% Fe, the XRD diffractograms and the UV-DR spectra show that CAT 40-Fe-650 and CAT 50-Fe-650 are quite similar to one another, and the TPR experiments show that the number of reducible species below 700 ºC is quite alike in both catalysts (see Table 2). Furthermore, the BET areas of both solids are very similar, so in principle an increase of the activity should be expected as the total Fe mass increases. However, this does not happen, and both catalysts have the same conversion curve. As already discussed above, at these high Fe loads amorphous Fe_2O_3 particles can be formed, which are undetectable by XRD, and they would have low activity, therefore explaining why the activity does not increase with the load of these two catalysts.

As reported often for the Fe-zeolite system [5-7, 10, 13] and for alumina supported Fe catalysts [17] and assuming that the reaction is first order, the apparent activation energy (E_{app}) of the catalysts calcined at 650 ºC is shown in Table 3. It also includes the data of a pure unsupported Fe oxide catalyst. The linear regression of the ln k vs. 1/T plot was quite good in all cases ($R^2 > 0.99$). This supports the first order assumption for the decomposition of N_2O on the Fe/Al_2O_3 system calcined at 650 ºC. The apparent activation energy values vary between 181 and 158 kJ/mol, and they are within the ranges reported in the literature for the catalysts supported on zeolites, whose E_{app} vary typically between 129 kJ/mol [6] and 235 kJ/mol [7], with the range between approximately 150 and 190 kJ/mol as the one reported most frequently [see comparative Table in ref. 41]. It can therefore be assumed, in principle, that the active sites and the reaction mechanism are similar in both systems.

Table 3. Apparent specific rate constants (k) at 600 ºC and apparent activation energies (E_{app}) for the different catalysts calculated assuming a first order reaction.

Catalyst	k (mol/g cat·s·bar) x10^4	k (mol/g Fe·s·bar) x10^3	E_{app} (kJ/mol)
Fe_2O_3-650	0.820	0.117	145
CAT 10-Fe-650	4.673	5.140	185
CAT 20-Fe-650	7.226	4.335	164
CAT 30-Fe-650	5.907	2.559	163
CAT 40-Fe-650	5.175	1.811	170
CAT 50-Fe-650	4.172	1.414	159
CAT 10-Fe-900	1.639	1.639	245
CAT 20-Fe-900	1.136	0.586	221
CAT 30-Fe-900	1.115	0.371	209
CAT 40-Fe-900	1.498	0.374	195
CAT 50-Fe-900	2.472	0.494	161

As can be seen, except for the catalyst with the smallest load, CAT 10-Fe-650, the activation energy does not vary substantially with the Fe load, and it varies around 164 kJ/mol, which indicates that the nature of the active sites and the controlling step are not modified with increasing Fe loads in the catalysts calcined at 650 ºC. In the case of the catalyst with 10% Fe load the activation energy is greater, 184 kJ/mol. According to Pirngruber et al. [6], a high activation energy is associated with isolated Fe^{3+} type species or forming dimers, while the existence of species mainly of the oligonuclear iron cluster type generate catalysts with lower activation energy. With CAT 10-Fe-650 catalyst both the XRD and UV-DRS analysis point at a large concentration of highly disperse Fe species and a very low concentration of Fe species formed by larger clusters or crystals detectable by XRD. Therefore the low concentration of Fe_2O_3 clusters or particles in CAT 10-Fe-650 would account for the higher E_{app} found for this catalyst. Table 3 reports that the apparent activation energy of pure Fe_2O_3 is 145 kJ/mol, confirming that the existence of large size and high crystallinity Fe_2O_3 species is associated with a relatively low activation energy. On the other hand, and as expected, the value of the apparent specific

constant, k, expressed per gram of catalyst, follows the same trend seen in the conversion, passing by a maximum in the catalyst with 20% Fe load. However and if the apparent specific constant is expressed per gram of Fe loaded in the reactor, its value decreases with the increase of the Fe load over the whole range considered in this study. The latter is in agreement with literature, in the sense that the more active species are small clusters or oligomers with few Fe atoms, which are formed preferentially at low Fe loads. In relation to the activity of pure unsupported Fe_2O_3, Table 3 shows that the specific rate constant is much smaller than that of the supported catalysts, particularly when it is expressed per gram of Fe. This low activity can be explained mainly by the very low specific surface area of the Fe_2O_3 calcined at 650 ºC. Actually, as will be shown later, the main problem with unsupported Fe_2O_3 is that it is sintered strongly as the calcination temperature increases, making it inapplicable as a catalyst at high temperatures.

The conversion vs. temperature data of the catalysts calcined at 900 ºC are shown in Figure 4(B). It is seen that when the catalysts are calcined for an additional period of 3 h at 900 ºC, all of them decrease their activity with respect to that seen when they are calcined at 650 ºC. The new activity sequence of the catalysts calcined at 900 ºC is: 50% > 10% ≈ 40% > 30% ≈ 20%.

As commented earlier, the catalyst with 50% Fe load is the most active when calcined at 900 ºC, because it is the least deactivated catalyst when it is calcined between 650 and 900 ºC. The XRD analysis of CAT 50-Fe-650 and CAT 50-Fe-900 catalysts show that the main change is the transformation of the support from γAl_2O_3 (calcined at 650 ºC) to α-Al_2O_3 (calcined at 900 ºC). There is also a small increase in crystallite size, as shown in Table 1. The UV-DRS of Figure 2 show that the spectra of CAT 50-Fe-650 and CAT 50-Fe-900 are similar to each other, except for a slight decrease of the Fe^{3+} species isolated when calcining at 900 ºC, indicating that the relative concentration of the Fe species does not change substantially upon calcining between 650 and 900 ºC. On the other hand, the reducibility of both catalysts is quite similar, as shown in Figure 3 and in Table 2. In fact, the maxima of the reduction temperature of the α peak differ by only 20 ºC, and the consumption of H_2 below 700 ºC is basically the same. Furthermore, it is also this catalyst the one that undergoes the smallest specific surface area loss as the calcination temperature increases, varying from 75 m^2/g to 33 m^2/g when calcined between 650 and 900 ºC. All the above, account for the low deactivation experienced by this catalyst when calcined at high temperature.

In the case of the catalyst with 40% load, the UV-DR spectra of Figure 2 show that calcination between 650 and 900 ºC does not produce substantial changes in the relative concentration of the Fe species. On the other hand, the reducibility of the catalyst decreases more than in the catalyst with greater load, because the maximum of the α peak is displaced 40 ºC to higher temperature by calcination at 900 ºC, as seen in Figure 3. The total reducible species below 700 ºC, however, practically do not vary by calcination at 900 ºC, as seen in Table 2. What does change strongly with the calcination at 900 ºC is the specific surface area. In fact, it decreases from 74 m^2/g when it is calcined at 650 ºC, down to only 17 m^2/g when calcined at 900 ºC. Therefore, the greater reduction of the activity of the catalysts with 40% Fe compared to those with 50% load can be attributed mainly to a higher reduction of the catalyst's specific surface area.

Something similar occurs with the catalysts with 30% Fe. The UV-DR spectra show a decrease of the relative concentration of the isolated Fe^{3+} species, while the other species do not change their concentration substantially. The reducibility decreases with the increase of the calcination temperature, and this is reflected in the reduction temperature maxima as well as in the total consumption of H_2 below 700 ºC. Again, the characteristic that undergoes the largest change upon calcination between 650 ºC and 900 ºC is the BET area, which is reduced from 76 m^2/g in CAT 30-Fe-650 to 12 m^2/g in CAT 30-Fe-900. In short, the changes undergone by this catalyst when calcined at 900 ºC point to a decrease of the catalytic activity, which actually takes place, but it is the specific surface area that undergoes the largest change when calcined at 900 ºC.

In the catalyst with 20% Fe, again the UV-DR spectra show that the concentration of Fe species does not vary substantially with the calcination between 650 and 900 ºC. The TPR experiments do show that the reducibility of the Fe species changes when it is calcined at 900 ºC. According to Table 2, the consumption of H_2 decreases by only 70% of that at 650 ºC. Furthermore, the loss of specific surface area is the largest in the series of catalysts studied reaching only 9 m^2/g after calcining at 900 ºC. The sum of these effects can explain why this is the catalyst with the lowest activity after calcination at 900 ºC.

Finally, the catalyst with 10% Fe does show a change in the concentration of Fe species, particularly the isolated Fe^{3+} species, which decrease upon calcination at 900 ºC. However, the concentration of bulk Fe_2O_3 species does

not increase substantially, as seen in the UV-DR spectra of Figure 2. The same can be deduced from the XRD analyses of Figure 1(B), which do not show diffraction peaks attributable to α-Fe_2O_3 when calcining at 900 ºC. The TPR analysis also shows a decrease of the catalyst's reducibility as the calcination temperature increases. On the other hand, the specific surface area of CAT 10-Fe-900 is the second largest of the catalysts calcined at 900 ºC. The lack of formation of bulk Fe_2O_3 species and the high specific surface area of this catalyst can explain why its activity is not reduced substantially when calcining at 900 ºC. In fact, CAT 10-Fe-900 is second in the activity sequence of the catalysts calcined at 900 ºC.

At present it is difficult to tell which is the characteristic that has the largest influence on the activity of the Fe catalysts supported on alumina, and further work is required to isolate them and quantify their real contribution. However, with the current information it can be seen that the activity sequence correlates well with the specific surface area sequence of the catalysts. In fact, the specific area sequence of the catalysts calcined at 900 ºC is CAT 50-Fe-900 ≈ CAT 10-Fe-900 > CAT 40-Fe-900 > CAT 30-Fe-900 ≈ CAT 20-Fe- 900, which agrees with the activity sequence reported earlier. A similar conclusion was reported by Giecko et al. [15] for catalysts prepared by coprecipitation of the precursors of Fe and Al and calcined at 900 ºC and 1100 ºC.

Table 3 also shows how the apparent activation energy varies with the Fe load in the catalysts calcined at 900 ºC. The first thing that stands out from the results of Table 3 is that the calcination leads to an increase of the reaction's apparent activation energy, with this increase being larger at lower Fe loads. The fact that the increase of the calcination temperature between 650 and 900 ºC also causes a change in the crystal structure of the alumina makes it difficult to assign the activation energy increase only to changes in the types of Fe species present on the surface of the alumina. This is an issue that should be included in coming studies. However, the effect of the Fe load on the catalysts calcined at 900 ºC can be interpreted on the basis of changes of the concentration of the different Fe species. In fact and in contrast with the catalysts calcined at 650 ºC, the apparent activation energy decreases with increasing Fe load from 245 kJ/mol in CAT 10-Fe-900 to 161 kJ/mol, in CAT 50-Fe-900. As discussed earlier, the apparent activation energy should decrease as the Fe particle size increases, because larger Fe clusters favor oxygen recombination on the surface. XRD diffraction shows that the concentration of crystalline Fe particles increases as the Fe load increases in the catalysts calcined at 900 ºC, explaining the decrease of the apparent activation energy.

In relation to the value of the apparent specific constant, and as expected, when it is expressed per unit of catalyst mass, it follows the same trend as the conversion, passing by a minimum in the catalyst with 30% load and then reaching its highest value in the catalyst with 50% Fe. When the apparent specific constant is expressed per gram of Fe in the reactor, the situation changes, the constant decreases between 10% and 40% of the Fe load, and then it increases slightly in the catalyst with 50% Fe. It should be noted that in every case the highest value of the specific constant is found for the catalyst with the lowest Fe load, confirming the greater activity of the highly dispersed Fe species. Table 3 also shows that the unsupported Fe_2O_3 calcined at 900 ºC does not present catalytic activity below 600 ºC. This is consistent with the high sintering of Fe_2O_3, generating a solid with a very low specific surface area, as shown in Table 1. This makes it necessary to support the Fe_2O_3 on alumina to obtain an active catalyst after precalcining at 900 ºC.

It must be stressed that selecting the calcination temperature as 900 ºC has the purpose of studying whether the alumina supported Fe catalysts can be used at high temperatures in the process-gas option. Although the activity decreases by calcining at 900 ºC, the catalysts still retain a substantial activity that is closed to the one reported by Giecko et al. [15], which makes this catalyst a good candidate for the elimination of N_2O at high temperatures.

Further studies on activity and stability in streams of non-ideal mixtures of gases present in the NH_3 oxidation reactor, at high temperatures, must be carried out before validating this system as a commercial catalyst to be used in the industrial process of nitric acid production.

4. CONCLUSIONS

This study shows that catalysts of Fe supported on alumina have high catalytic activity if they are calcined at moderate temperatures (650 ºC). It was found that the activity is dependent on the amount of Fe, showing an optimum Fe loading close to 20%. This catalyst presents 97% N_2O conversion at 600 ºC.

When calcined at a high temperature (900 ºC), the activity decreases, but this decrease is dependent on the Fe load. The determining factor in the activity of the catalysts calcined at 900 ºC seems to be their specific surface area. In fact, the most active catalyst after a treatment at high temperature is the

one with the largest Fe load, 50%, which presents the largest specific surface area. That same catalyst presents an N_2O conversion (at 600 ºC) of 89% when calcined at 650 ºC, but it decreases to 77% when calcined at 900 ºC.

The high activity observed after calcining the catalyst at 650 °C and that retained when calcined at 900 °C, makes the alumina-supported iron catalyst a good candidate to be used in the process-gas option for eliminating N_2O from nitric acid production plants.

ACKNOWLEDGMENTS

REFERENCES

1.- G. Centi, S. Perathoner, F. Vanazza, M. Marella, M. Tomaselli, M. Mantegazza, Adv. Environ. Res. 4 (2000) 325-338.
2.- M. Hevia, J. Pérez-Ramírez, Applied Catalysis B 77 (2008) 248-254.
3.- E. Malki, R. van Santen, W. Sachtler, J. Catal. 196 (2000) 212-223.
4.- B. Wood. J. Reimer, A. Bell, M. Janicke, K. Ott, J. Catal. 224 (2004) 148-155.
5.- K. Sun, H. Xia, E. Hensen, R. van Santen, C. Li, J. Catal. 238 (2006) 186-195.
6.- G. Pirngruber, P. Roy, R. Prins, J. Catal. 246 (2007) 147-157.
7.- L. Pirutko, V. Chernyavsky, E. Starokon, A. Ivanov, A. Kharitonov, G. Panov, Applied Catalysis B 91 (2009) 174-179.
8.- M. Rivallan, G. Ricchiardi, S. Bordiga, A. Zecchina, J. Catal. 264 (2009) 104-116.
9.- P. Sazama, N. Sathu, E. Tabor, B. Wichterlova, S. Sklenak, Z. Sobalik, J. Catal. 299 (2013) 188-203.
10.- G. Panov, V. Sobolev, A. Kharitonov, J. Mol. Catalysis 61 (1990) 85-97.
11.- G. Pirngruber, M. Luechinger, P. Roy, A. Cecchetto, P. Smirniotis, J. Catal. 224 (2004) 429-440.
12.- I. Yuranov, D. Bulushev, A. Renken, L. Kiwi-Minsker, J. Catal. 227 (2004) 138-147.
13.- E. Kondratenko, J. Pérez-Ramírez, Journal of Physical Chemistry B 110 (2006) 22586-22595.
14.- A. Heyden, B. Peters, A. Bell, F. Keil, Journal of Physical Chemistry B 109 (2005) 1857-1873.
15.- G. Giecko, T. Borowiecki, W. Gac, J. Kruk, Catalysis Today 137 (2008) 403-409.
16.- J. Kruk, K. Stolecki, K. Michalska, M. Konkol, P. Kowalik, Catalysis Today 191 (2012) 125-128.
17.- P. Pomonis, D. Vattis, A. Lycourghiotis, C. Kordulis, J. Chem. Soc. Faraday Trans. 1, 81 (1985) 2043-2051.
18.- C. Kordulis, H. Latsios, A. Lycourghiotis, P. Pomonis, J. Che. Soc. Faraday Trans. 86 (1990) 185-187.
19.- S. Christoforou, E. Efthimiadis, I. Vasalos, Catalysis Letters 79 (2002) 137-147.
20.- G. Pekridis, C. Athanasiou, M. Konsolakis, I. Yentekakis, G. Marnellos, Top. Catal. 52 (2009) 1880-1887.
21.- M. Colaianni, P. Chen, J. Yates, Surface Science 238 (1990) 13-24.
22.- Z. Zhong, T. Prozorov, I. Felner, A. Gedanken, Journal of Phys. Chem. B 103 (1999) 947-956.
23.- Z. Li, J. Sheng, Y. Wang, Y. Xu, Journal of Hazardous Materials 254-255 (2013) 18-25.
24.- J. Pérez-Ramírez, M. Kumar, A. Bruckner, Journal of Catalysis 223 (2004) 13-27.
25.- E. Berrier, O. Ovsitser, E. Kondratenko, M. Schwidder, W. Grunert, A. Bruckner, Journal of Catalysis 249 (2007) 67-78.
26.- A. Koekkoek, W. Kim, V. Degirmenci, H. Xin, R. Ryoo, E. Hensen, Journal of Catalysis 299 (2013) 81-89.
27.- M. Nechita, G. Berlier, G. Martra, S. Coluccia, F. Arena, G. Italiano, G. Trunfio, A. Parmaliana, Il Nuovo Cimento B 123 (2008) 1541-1551.
28.- M. Tepluchin, D. Pham, M. Casapu, L. Madler, S. Kureti, J. Grunwaldt, Catal. Sci. Technol. 5 (2015) 455-464.
29.- O. Wimmers, P. Arnoldy, J. Moulijn, Journal of Physical Chemistry 90 (1986) 1331-1337.
30.- M. Tiernan, P. Barnes, G. Parkes, Journal of Physical Chemistry B 105 (2001) 220-228.
31.- A. Venugopal, J. Aluha, D. Mogano, M. Scurrell, Applied Catalysis A 245 (2003) 149-158.
32.- W. Jozwiak, E. Kaczmarek, T. Maniecki, W. Ignaczak, W. Maniukiewicz, Applied Catalysis A 326 (2007) 17-27.
33.- J. Zielinski, I. Zglinicka, L. Znak, Z. Kaszkur, Applied Catalysis A 381 (2010) 191-196.
34.- P. Michorczyk, P. Kustrowski, L. Chmielarz, J. Ogonowski, Reaction Kinetics Catalysis Letters 82 (2004) 121-130.
35.- H. Zhou, Y. Su, W. Liao, W. Deng, F. Zhong, Applied Catalysis A 505 (2015) 402-409.
36.- J. Peréz-Ramírez, F. Kapteijn, A. Bruckner, Journal of Catalysis 218 (2003) 234-238.
37.- T. Nobukawa, M. Yoshida, K. Okumura, K. Tomishige, K. Kunimori, Journal of Catalysis 229 (2005) 374-388.
38.- P. Sazama, B. Wichterlova, E. Tabor, P. Stastny, N. Sathu, Z. Sobalik, J. Dedecek, S. Sklenak, P. Klein, A. Vondrova, Journal of Catalysis 312 (2014) 123-138.
39.- J. Wang, H. Xia, X. Ju, Z. Feng, F. Fan, C. Li, Journal of Catalysis 300 (2013) 251-259.
40.- T. Vulic, A. Reitzmann, K. Lazar, Chemical Engineering Journal 207-208 (2012) 913-922.
41.- G. Moretti, G. Fierro, G. Ferraris, G. Andreozzi, V. Naticchioni, Journal of Catalysis 318 (2014) 1-13.